European Rotorcraft Forum

TRACKING DYNAMICALLY SCALED SEPARATING OBJECTS DURING A HELICOPTER WIND TUNNEL TEST

Anton de Bruin*, anton.de.bruin@nlr.nl; Karel Lammers*, karel.lammers@nlr.nl;
Iwan Philipsen**, iwan.philipsen@dnw.aero; Jos Postma**, jos.postma@dnw.aero;
Minhyoung Ryu***, minhyoung.ryu@koreaaero.com
*NLR, **DNW, ***KAI

Abstract
A wind tunnel test was made to investigate safe dropping of objects from a helicopter, as might be needed during emergency situations. For a correct simulation of the object trajectory, Froude scaling was used, which also required a proper dynamic scaling of the object mass, center of gravity at mass inertia. A rapid prototyping manufacturing technique was used for the dropped objects. On the dropped objects a unique pattern of fluorescent markers was applied and the position of the individual markers was determined by a Stereo Pattern Recognition technique, using two high speed (500 Hz) cameras. Post-processing of these camera images provided detailed information on the object trajectory and the object attitude angles, which were the prime purpose of the tests. With detailed trajectory data available an attempt was made to derive the aerodynamic forces and moments on the object during its fall. This application requires high accuracy of the trajectory data, which could not be reached with the test setup chosen. The paper presents the test setup and model and then focusses on the trajectory measuring system used, the results obtained and a discussion on how the trajectory measurement accuracy might be improved.

1. INTRODUCTION

1.1. General introduction

In some emergency cases it is necessary to drop an object from an aircraft. The conditions, under which an object can be safely dropped, without the risk to impact the aircraft, need to be investigated. Wind tunnel tests can be effective to assess the flight operation safety margins, provided proper scaling rules are obeyed and accurate tracking of the object can be performed.

The Korea Aerospace Industries Co. LTD (KAI) develops a wide range of helicopters. KAI contracted the Netherlands Aerospace Centre (NLR) to measure trajectories from emergency released objects, dropped from a 1:8.5 scaled helicopter wind tunnel model. Tests were performed at the Low-Speed Tunnel (LST) of the German-Dutch Wind Tunnels (DNW) using an optical tracking system. The paper considers the tracking of such objects in the wind tunnel.

1.2. Scaling laws

The trajectory of an 1:8.5 geometrically scaled object represents the trajectory of the full scale object, only if all forces acting on the object scale proportional [1]. In this experiment these forces are gravity (Fg) and aerodynamic (Fa) forces only, hence:

(1) $$Fg_{fs}/Fg_m = Fa_{fs}/Fa_m$$

The subscripts fs and m denote the full scale and model scale respectively.

Since low Mach number conditions (M<0.25) apply here, compressibility effects are minor and Froude scaling is appropriate [2]. The Froude similarity parameter (*Fr*) is defined as:

(2) $$Fr = V/\sqrt{gL}$$

, where V is a characteristic flow velocity, *g* is the gravitational acceleration and *L* is a characteristic length of the model. For maintaining a constant value for *Fr* between full scale and subscale wind tunnel test (scale factor $\lambda = L_{fs}/L_m = 8.5$), the wind tunnel speed has to be reduced:

(3) $$V_m = V_{fs}/\sqrt{\lambda}$$

In a similar way, with Froude scaling, the scaling of other relevant parameters can be derived, as given in Table 1.

Table 1. Relevant scaled parameters.

Geometry	$L_m = \lambda^{-1} \cdot L_{fs}$
Mass	$m_m = \lambda^{-3} \cdot m_{fs}$
Mass inertia	$I_{ij,m} = \lambda^{-5} \cdot I_{ij,fs}$
Ejector force	$Fe_m = \lambda^{-3} \cdot Fe_{fs}$
Aerodynamic force	$Fa_m = \lambda^{-3} \cdot Fa_{fs}$
Flow velocity	$V_m = \lambda^{-1/2} \cdot V_{fs}$
Body velocity	$U_m = \lambda^{-1/2} \cdot U_{fs}$
Acceleration	$a_m = a_{fs}$
Angular velocity	$\dot{\theta}_m = \lambda^{1/2} \cdot \dot{\theta}_{fs}$
Angular acceleration	$\ddot{\theta}_m = \lambda \cdot \ddot{\theta}_{fs}$
Time	$t_m = \lambda^{-1/2} \cdot t_{fs}$

The full scale helicopter has a passive release mechanism, therefore Fe=0. For the remainder of this paper dimensions are given in model scale.

Presented at 44th European Rotorcraft Forum, Delft, The Netherlands, 19-20 September, 2018

2. TEST SET-UP

2.1. General

Since main focus of the tests was on forward flight conditions, the influence of a rotor was considered to be small and therefore a 1:8.5 scaled helicopter wind tunnel model without rotor was used for the test. Tests were performed in the low speed DNW-LST wind tunnel, having a test section cross section of 2.25x3 m^2. The model was suspended from the ceiling of the test section. Objects were released from the model for different model angle of attack and side-slip conditions. It should be noted that, strictly speaking, under horizontal flight non-zero angle of attack conditions the direction of the gravitation vector was incorrect with respect to the flow vector (correct testing would require a tilted wind tunnel circuit).

Two types of objects were manufactured and tested, here referred to as object #1 and object #2. During the tests the objects can have different loading configurations (empty or (partially) loaded), each having its requested own mass, CoG and mass inertia characteristics. Only completely full or completely empty configurations will be discussed in this paper. Object #1 has a cylindrical shape and object #2 has a more complicated shape with two interconnected horizontally parallel cylinders. A schematic view of the objects is shown in Figure 1. The boxes enclosing the objects have only been added for later data presentation of object trajectories.

The floor of the test section was covered with acoustic foam to prevent the object to be damaged. A flexible net was placed downstream to prevent the object from being blown too far downstream. Before the test, a dedicated test section calibration was made for the presence of the foam and net.

A non-intrusive optical measurement system, based on stereo pattern recognition (SPR), was used to measure all 6 degrees of freedom (DOF) movements of the dropped object along its trajectory.

2.2. Design and manufacturing of the objects and their verification

The objects are highly detailed in shape and of low weight and have therefore been (partly) manufactured with state-of-the-art rapid prototyping. Detailed iterative CAD design was needed to comply with the mass, center of gravity location and the mass inertia scaling rules given in Table 1. The Froude scaled mass of the objects was in the range between 25 and 170 grams. After manufacturing the objects, their mass and CoG was carefully checked with two high precision (0.01 gram) laboratory scales, see Figure 2. Deviations between Froude scaled masses and actual masses of the objects were found to be less than 1%.

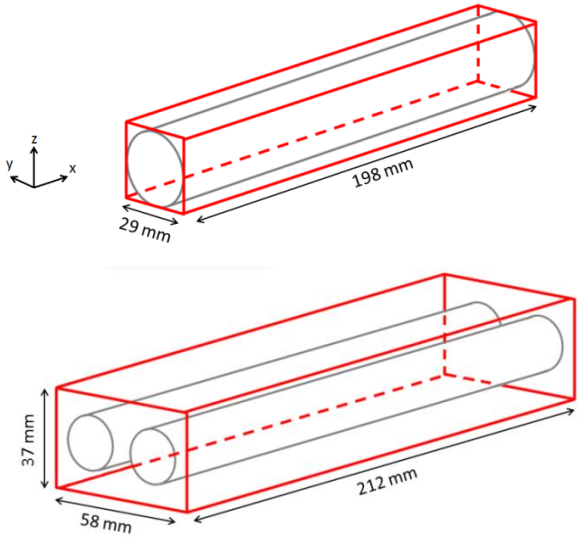

Figure 1. Schematic view of object #1 (top) and object #2 (bottom) with enclosing boxes (dimensions in model scale, front side to the left).

Figure 2. Measuring mass and CoG.

A bifilar torsional pendulum method [3], with the object hung between two parallel filaments and optical tracking of markers, was used to determine the rotational mass inertia from the equation of motion for a pendulum. The oscillating motion was captured with 200 frames per second, using a high speed camera. The results of the conventional linear approximations were compared to the results using the non-linear equation of motion of the oscillator. The non-linear method takes account of the damping effects of the pendulum moving in air [4]. The longitudinal mass inertia of the manufactured objects was found to be within 4% accuracy with respect to its requested value [5]. The mass inertia around the longitudinal axis was not checked, because the relatively short horizontal distance between the two parallel filaments of the pendulum would cause relatively high measurement errors.

Presented at 44th European Rotorcraft Forum, Delft, The Netherlands, 19-20 September, 2018

2.3. Release of the objects

A zero reaction force release of the objects was requested for the wind tunnel model to replicate the full scale situation. On the full size helicopter two release clamps are used, which could not be realized in the reduced sized wind tunnel model. Instead a reaction force free release hook mechanism was designed. The release hook and release clamps are shown in Figure 3. The working principle of the release hook is depicted in Figure 4. The full scale release clamps are passively incorporated in the wind tunnel model, which is important because the object may touch the clamps right after release, thereby influencing the trajectory. The release hook, positioned between the release clamps, is operated by a push rod as shown in Figure 4.

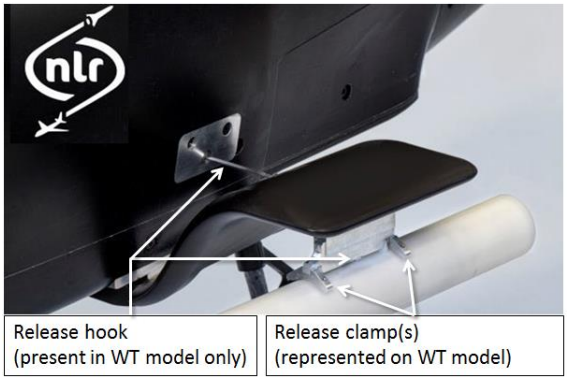

Figure 3. Full scale and model scale release mechanism.

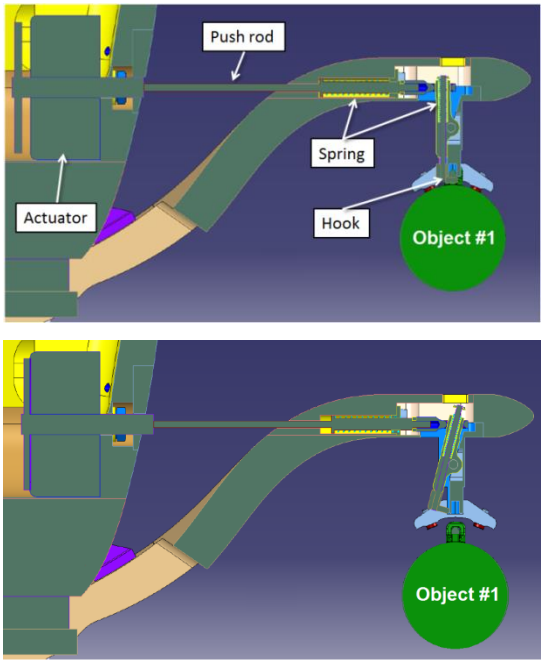

Figure 4. Release mechanism just before release (top) and just after release (bottom).

2.4. Trajectory measurement

The general test setup is shown in Figure 5

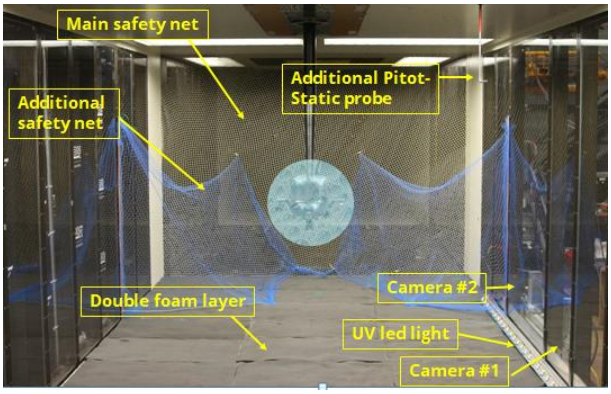

Figure 5: Test setup in DNW-LST wind tunnel.

The object trajectories are captured with a two-camera Stereo Pattern Recognition measurement technique [6]. The SPR measurement equipment consisted of two Mikrotron EoSens CoaXPRess 4CXP 4 Megapixel cameras (2336x1728 pixel) with 12 mm Kowa objective lenses and an adapted computer with software and equipment. The DNW-LST wind tunnel offers good optical access through the tunnel side walls (see Figure 5). The camera arrangement has been chosen such as to observe a pre-defined volume around the helicopter for tracking the objects. Prior to the drop tests, the camera set-up is calibrated by placing a calibration frame (Figure 6) in the wind tunnel. This allows determination of the marker locations in the wind tunnel coordinate system. The uncertainty in determination of individual marker locations is estimated at 0.025 mm in x- and z-direction, and 0.06 mm in y-direction. The larger uncertainty for the y-directions is due to the chosen two camera arrangement. A right hand coordinate system is used. The x-direction is in stream wise direction, the z-direction in vertical direction (upward positive) and y-direction is in lateral direction (see also Figure 1).

Figure 6. Calibration frame for SPR system.

Presented at 44th European Rotorcraft Forum, Delft, The Netherlands, 19-20 September, 2018

On the objects a unique pattern of fluorescent markers is applied. Suppose the total number of markers is N. Prior to the test, the position of the marker centers has been measured on a position measurement machine. These coordinates are given in a local object oriented coordinate system. During object tracking, the wind tunnel is illuminated by UV light only. Filters on the camera lenses ensure that only light of the wavelength reflected by the markers is entering the cameras. When the model and wind tunnel conditions are set, the following automated sequence was executed for recording the trajectories. Wind tunnel illumination was dimmed and a high-power UV-light source was activated to generate sufficient light intensity and contrast for marker detection by the camera system during a short lens opening time of the cameras. A trigger sequence starting the acquisition of 500 frames at a rate of 500 Hz (1 s of data with Δt= 0.002 s) was initiated together with the activation of the release mechanism of the object. One second of data was recorded, whereas a typical object observation duration in the cameras is only about 0.4 s. Using the SPR system and a marker on the release hook, it has been established that about three frames are already recorded before full retraction of the release hook (and release of the object) is established. Therefore also the initial location and attitude of the object, while still attached to the helicopter, is recorded during the measurement.

A sequence of recorded images ($\Delta t \approx$ 0.024 s) for one of the cameras is given in Figure 7. Figure 8 shows the complete sequence of compiled images (Δt=0.002 s), clearly showing that individual markers can be tracked throughout the complete trajectory. Some markers have been placed on the helicopter fuselage and a reflective tape has been place around the wheel, for easy reference.

Note that individual marker images vary in intensity and shape, depending on the observation angle and their illumination. In particular it seems that the illumination in the right bottom corner of the observation area is less optimal and that the finite shutter speed of the cameras (0.001s) seems to result in elongated markers during the final part of the trajectory when markers move with relatively large velocity (see Figure 8).

Figure 10 presents a zoom-in pixel representation of markers, clearly showing the limited pixel resolution of the cameras used.

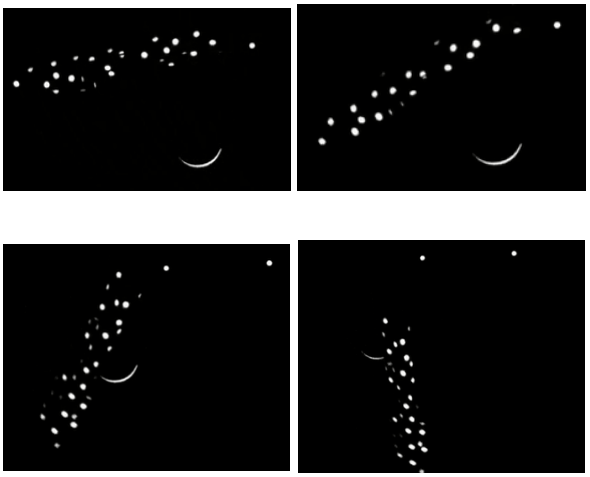

Figure 7: Sequence of zoomed and clipped camera images, showing the markers on object #1 and background reference markers on wheel contour and helicopter fuselage.

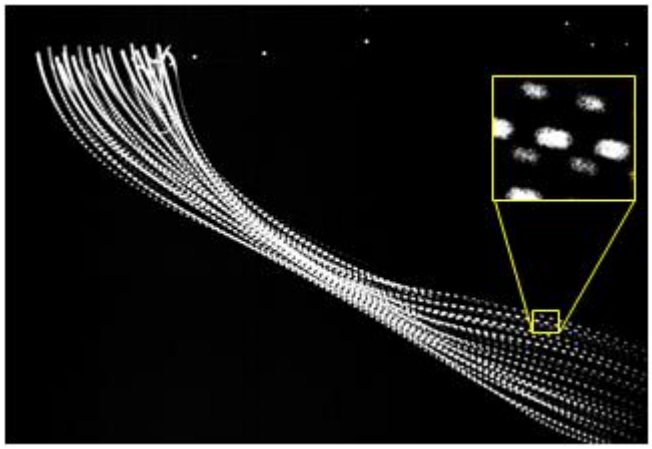

Figure 8: Combined (merged) camera images after release of object #1.

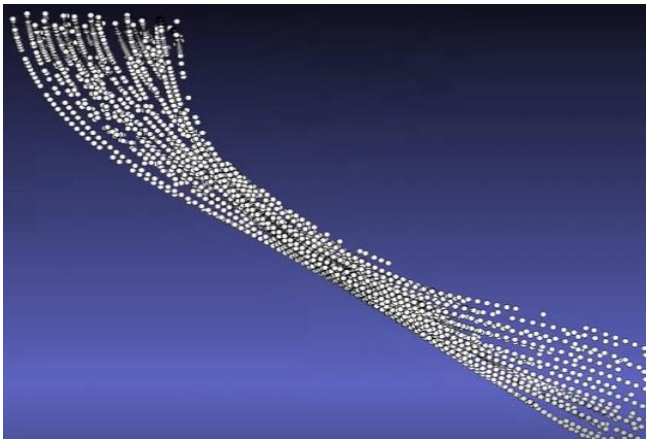

Figure 9: Evaluated marker positions from the two cameras. Same data as in Figure 7.

Presented at 44th European Rotorcraft Forum, Delft, The Netherlands, 19-20 September, 2018

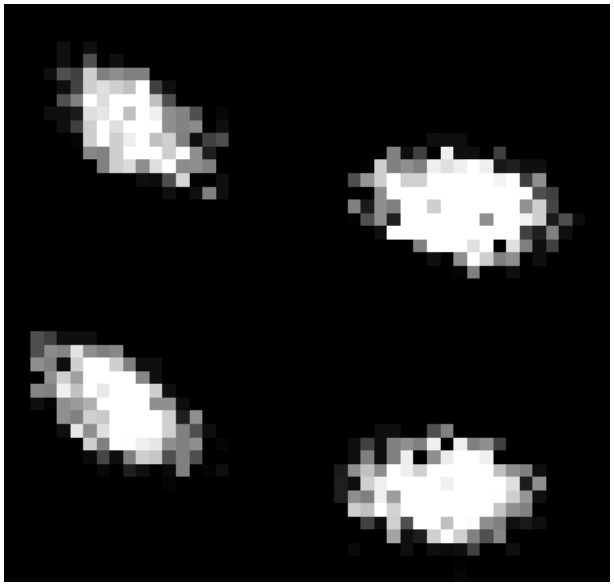

Figure 10: Zoomed-in image showing pixel representation of some markers

It should be noted that the model was illuminated only from the bottom corner of the test section (as visible at the wheel), leaving some of the markers on topside of the object less visible.

In order to establish the position and attitude of the object at each time instant, the camera images are processed as illustrated in Figure 11.

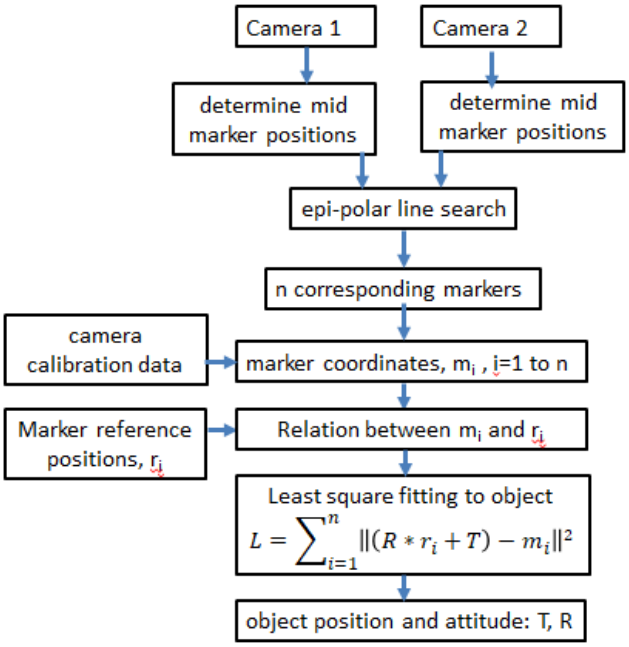

Figure 11: Camera data processing steps

In the first processing step a threshold level filtering is used to retain only pixel light intensities above 40 (255 is the maximum value for the used cameras), subsequently a 3x3 pixel Gausian filtering has been used to gain a more smoothed

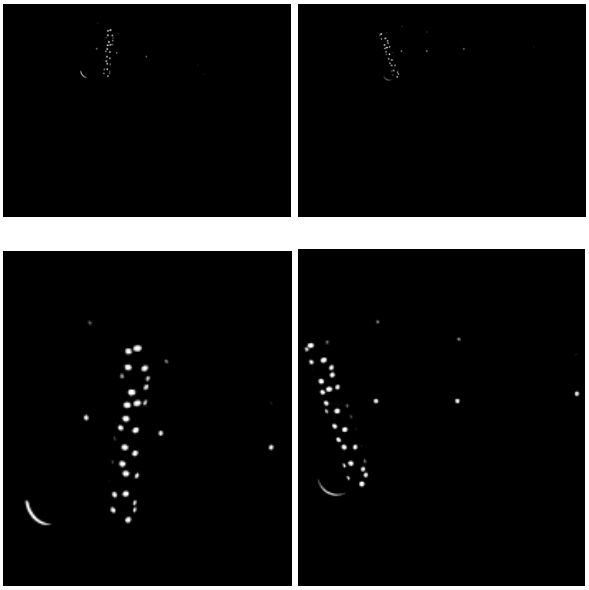

Figure 12: Camera images for a certain time instant. Camera #1 left, camera #2 right. Original images top, zoomed images bottom.

marker image, then the mid position of each isolated marker is computed in camera pixel coordinates. This is followed by an epi-polar line search to establish corresponding markers in each camera image.

An example of camera images at a certain time instant is shown in Figure 12. The epi-polar line search process returns n corresponding markers (with n in general less than ½N, where N is the total number of markers on the object). However, it generally will also yield some ghost marker positions not belonging to the object.

As can be seen in Figure 9, the epi-polar line search may result in incomplete trajectories for individual markers, though the sequence of individual marker images may be complete in each camera (compare with Figure 8). Based on the camera calibration data it is now possible to translate the camera pixel coordinates of the n corresponding markers to actual coordinate vectors m_i in wind tunnel coordinate system. This incomplete and randomly ordered marker list is input to a software module that identifies the identification number of each marker m_i with that of the known reference marker coordinate vectors r_i. The final processing step is to determine the position and orientation of the store, using a least square algorithm, with L the function to be minimized, *R* the 3x3 rotation matrix and T a translation vector. R and T are the outcome of the minimization process. The rotation matrix can be decomposed into an Euler angle sequence: a roll-pitch-yaw sequence was chosen. Performing this procedure for each time frame allows for a

Presented at 44th European Rotorcraft Forum, Delft, The Netherlands, 19-20 September, 2018

complete characterization of the store trajectory and attitudes.

The position vector in wind tunnel coordinates *p* of a certain local object reference coordinate position vector p_0 follows from:

(4) $$p = R * p_0 + T$$

This procedure was used to visualize the movement of the boxes around the object, as shown in Figure 1.

In general this data processing, fully based on individual image pairs, worked well. However, it should be noted that at least three markers should be simultaneously visible in both cameras ($n \geq 3$) in order to be able to compute the object position and attitude. Also, when having only few markers visible this will reduce the accuracy of the least square fitting process. By using just two cameras it is apparent that when the longitudinal axis of the object is closely aligned with the view axis of one of the cameras, the location of the markers cannot be established precise enough and there is the risk that one of the cameras observes just a few markers. In such a case the object can become "invisible" for the SPR system. This can be circumvented or improved by the use of three or four cameras.

Another potential risk is that the reference position of individual markers r_i on the object has been measured with insufficient accuracy. This may influence the established relationship between m_i and r_i (false identifications) and will degrade the quality of the least square fitting proces.

3. RESULTS AND ANALYSIS

The ultimate objective of the wind tunnel test is to explore the range of safe conditions to perform emergency store separation. This requires the accurate determination of the object trajectory and attitude. For some frames it was not possible to determine the position and attitude of the object, resulting in 'missing frames' in the trajectory.

Trajectory results for the relatively light empty object #1, for which aerodynamic forces and moments are relatively dominant, are shown as example. For the test cases shown the airspeed is 16 m/s (Froude scaled). Only the first 0.3 seconds of the drop are shown in order to maintain axis ranges that still make it possible to distinguish differences between runs. For confidentiality reasons no values on the vertical axis are shown, but only scale range is indicated.

Figure 13 compares two test results for nominal identical test conditions, where the object does not hit the helicopter. In this case a very good reproducibility in trajectory and object attitude angles is achieved. Similar reproducibility results are obtained with other repeat runs. This demonstrates proper functioning of the release mechanism, a proper measurement technique and quite stable flow conditions around the helicopter. In general the trajectory data show a smooth behavior. Closer inspection reveals that at some time frames the image processing was not able to derive trajectory data. Gaps in the data sequence can be observed at t<0.02 s and especially sparse data occur in the region between t=0.23 and 0.28. In a few cases trajectory data do not fit with the general trend, pointing to a false data point. The precise reason for this is not known, it would require a detailed analysis of the intermediate data processing steps.

Figure 14 shows that the differences in trajectory and attitude data between these two repeat runs, slowly increase. It should be noted that the scatter in these subtracted data is roughly twice that of the original data sets. Neglecting obviously false data points it can be concluded that the data are quite smooth, except for the roll angle data. The latter is explainable because it is evaluated from marker distances less than the diameter of the object, whereas the other attitude angles are evaluated from marker positions over the full length of the object.

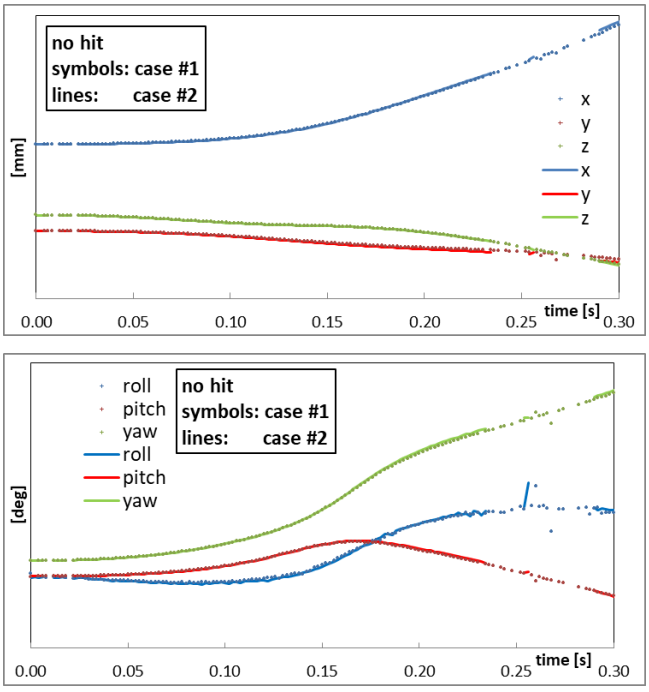

Figure 13. Object trajectory and attitude as function of test time for two repeat tests, where the object does not hit the helicopter model. Vertical scale range is 1200 mm and 400 deg.

Presented at 44th European Rotorcraft Forum, Delft, The Netherlands, 19-20 September, 2018

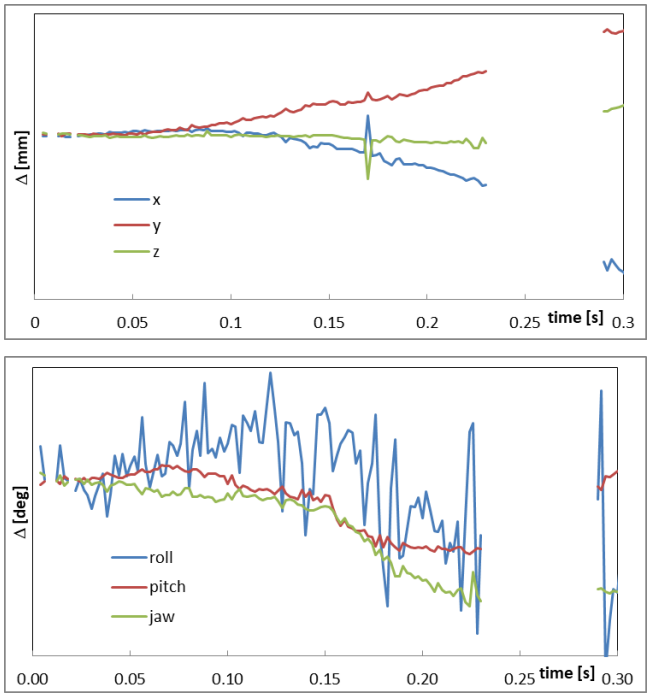

Figure 14: Difference between object trajectory and attitude data of two repeat runs, when object does not hit the helicopter. Vertical scale range is 35 mm and 10 deg.

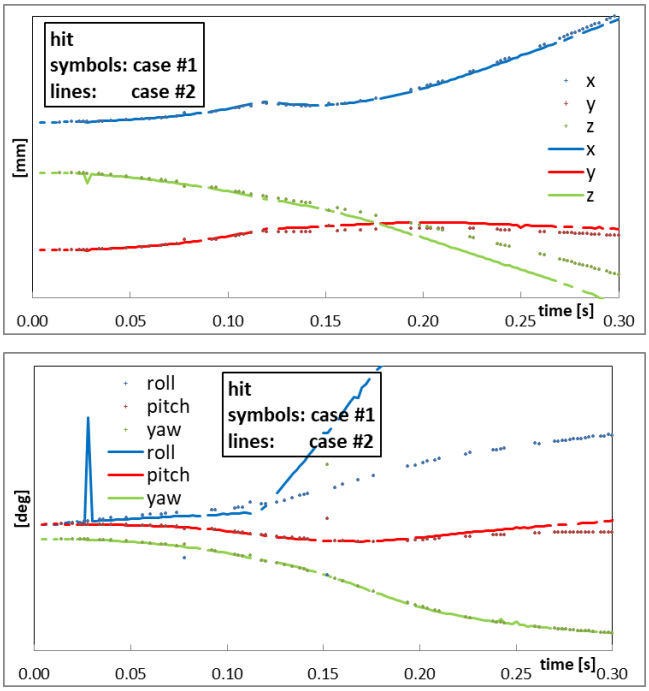

Figure 15. Object trajectory and attitude as function of test time for two repeat tests, where object hits the helicopter model. Vertical scale range is 800 mm and 450 deg.

Figure 15 compares two repeat measurements with nominal identical test conditions, where the object just hit the main landing gear of the helicopter. It should be noted that the determination of safe object release operating conditions was the purpose of the test and that for establishing the safe boundaries quite unusual aircraft operating conditions had to be explored to make the released object hitting the helicopter. In both cases the released object just hit the nearby main landing gear of the helicopter model at about 0.12 s after release. In both cases it introduced a temporally stop in x movement of the object and a small kink in the y trajectory. For case #2 it also introduced a large roll spinning rate of the object after impact, whereas for case #1 this is not really visible. Such a strike of the object with the helicopter model can be identified from the processed trajectory results, but could also be identified directly after each test point when slowly replaying the SPR camera images, showing the movement of the markers. A marker was also placed on the landing gear to visualize it in the recordings (see Figure 7). This nearby model part was known to be a potential target for object impact. This strike identification approach with marker on the wheel increased the effectiveness of the test in terms of exploring safe separation condition ranges, see also Figure 16.

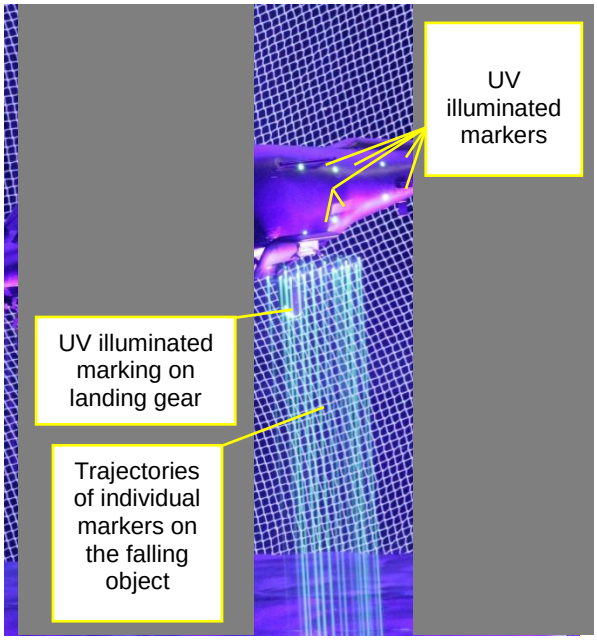

Figure 16: Photographic recording with long exposure time, markers on the model are clearly visible.

The Cartesian coordinates of the trajectories presented are the coordinates of the object reference point (which is not the CoG because of different object configurations tested). With this object reference point and the store orientation it is possible to construct the boxes of Figure 1 at every time frame, using equation 4.

Presented at 44th European Rotorcraft Forum, Delft, The Netherlands, 19-20 September, 2018

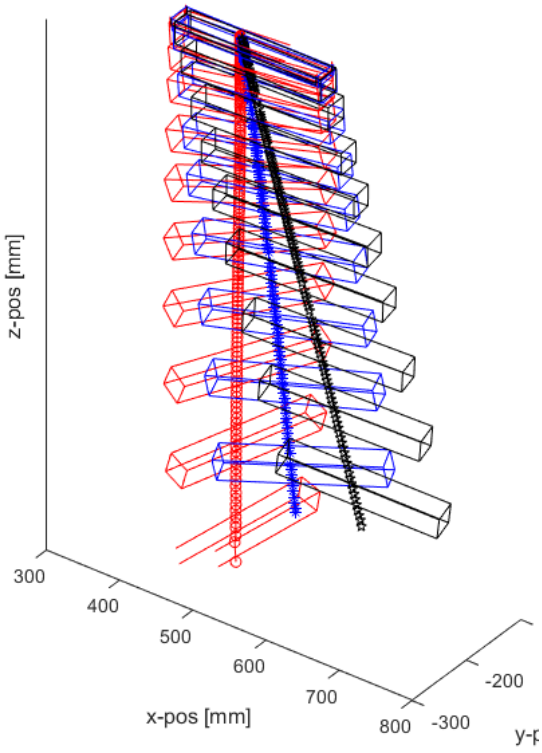

Figure 17. AoA-sweep of full object #1 box trajectory, alpha=10 (black), alpha=0 (blue), alpha=-10 (red).

An example to illustrate 3D-trajectories, depending on model angle of attack (alpha=-10, 0, + 10 deg), is shown in Figure 17. These are trajectories for the fully loaded object #1 configuration, which are therefore dominated by gravity. Nevertheless, the alpha dependent aerodynamic forces appear to induce a considerable effect on the pitch, yaw and roll motion of the object. At alpha=10 deg there is primarily a pitch up motion of the object, at alpha=0 and especially at alpha=-10 a considerable pitch down, yaw and roll motion sets in. The range of the vertical axis is roughly 1200 mm. The airspeed was 23 m/s and the trajectories are given in the helicopter aligned axis system.

It is tempting to further exploit the quantitative trajectory data. With known mass and inertia characteristics of the objects, it is in principle possible to derive aerodynamic forces and moments from the trajectory data, provided sufficiently reliable linear and angular accelerations of the object and thus 2nd order time derivatives of the trajectory data are available. Nevertheless an attempt was made. Firstly, Interpolation was needed to cover missing data points. Secondly, data outliers had to be repaired. Outliers were removed and replaced with fitted data points by using a moving average filter (with a stencil size of 5 frames). A data point was identified as outlier when the residue between data point and fitted value was more than 6 times the median value of all residues for that trajectory. Finally, smoothing was needed due to the limited accuracy of individual data points.

As reported in [7], general trends on aero load data were successfully captured for a limited set of trajectories. However, for most trajectories it was not possible to derive reliable aerodynamic forces and moments. This is mainly caused by the missing frames. The accuracy and redundancy of the technique needs further improvement before such an application becomes feasible and reliable.

4. CONCLUSIONS

KAI, NLR and DNW conducted a successful emergency store separation low speed wind tunnel test, using Froude dynamically scaled and 1:8.5 geometrically scaled objects dropped from a helicopter wind tunnel model.

Target mass, CoG and mass inertia were determined with Froude scaling of full scale objects. By making use of state-of-the-art 3D-modelling and rapid prototyping it was possible to manufacture objects that complied with the mass, CoG and mass inertia requirements.

The optical stereo pattern recognition system made it possible to observe and measure the trajectories of the store without causing any flow disturbance. With this measurement technique any direct impact of the object on the helicopter could be identified quickly, increasing the effectiveness of the test.

For the assessment of safe object release operating conditions, being the main goal of the tests, the trajectories were generally measured with satisfying accuracy.

An initial attempt was made to derive unsteady aerodynamic forces and moments from the trajectory data. Unfortunately, missing time frames required interpolation and this hampered a reliable evaluation. Also the minor scatting in trajectory results requires data to be smoothed before they can be used for computing aero loads.

Several improvements in the measurement technique seem possible.

Camera hardware improvements:

- Using higher resolution cameras
- Using cameras with larger light sensitivity, enabling to reduce camera opening time, thus diminishing the moving marker effects in the images

Presented at 44th European Rotorcraft Forum, Delft, The Netherlands, 19-20 September, 2018

- Using more cameras to observe the falling object from different directions

Other hardware related improvements:

- Apply illumination not only from the bottom corner of the test section, but also from the top corner, thus giving a better illumination of all markers in all camera line of sight conditions.

Data processing related improvements:

- Instead of applying single time frame processing, add more physics in the post-processing by handling the 6 DOF as a coupled system.
- Improve the supplied reference positions (r_i).of the markers. E.g. by measuring them more precisely with an optical scanning technique.

Data post-processing was performed partly by DNW and partly by NLR. DNW determined the trajectories in tunnel coordinate system. NLR smoothed and interpolated the data and provided trajectories in airframe oriented coordinate system. NLR also tried to derive the instantaneous aerodynamic forces and moments from these trajectories.

Currently NLR and DNW are considering and developing steps to further improve trajectory measurement.

References

[1] Schindel L H. Store separation. *AGARD-OGRAPH-202*, No. 202, 1975

[2] Deslandes R M and Donauer S. Scaled-Drop-Tests: WYSIWYG or Not?. *48th AIAA Aerospace Sciences Meeting*, pp 2010-681, 2010.

[3] Shakoori A, Betin A V and Betin D A. Comparison of three methods to determine the inertial properties of free-flying dynamically similar models. *Journal of Engineering Science and Technology*, Vol. 11, No. 10, pp 1360-1372, 2016.

[4] Jardin M R and Mueller E R. Optimized measurements of unmanned-air-vehicle mass moment of inertia with a bifilar pendulum. *Journal of Aircraft*, Vol. 46, No. 3, pp 763-776, 2009.

[5] Meulen M P. Determination of rotational inertia using the bifilar pendulum method. *NLR-TR-2016-486*, Netherlands Aerospace Centre (NLR), Marknesse, 2016.

[6] Postma, J., Artois, K. and Philipsen, I. Wind Tunnel Test on the Breakthrough Laminar Aircraft Demonstrator Europe in the DNW-LLF, *53rd AIAA Aerospace Sciences Meeting*, pp 2015-1561, 2015.

[7] Lammers K.H, Philipsen I., Ryu M.H.: Release of dynamically scaled objects from a helicopter wind tunnel model, ICAS 2018, Bello Horizonte, Brazil, September 9-14, 2018.

Presented at 44th European Rotorcraft Forum, Delft, The Netherlands, 19-20 September, 2018